A Temperature Prediction Model In New Concrete Pavement

Sungchul Yang, Senior Engineer
Korea Highway Corporation and Texas A&M University

Dan G. Zollinger, Associate Professor
Texas A&M University and Texas Transportation Institute

Robert O. Rasmussen, Vice President,
Transtec, Inc.

ABSTRACT

The interaction between temperature conditions in concrete structure within the first few days after the concrete is placed can influence the quality of the concrete over its lifetime. This means that process occurring in concrete at an early age have an important influence on concrete quality. Therefore, planning of concrete placement should account for monitoring of temperature as well as strength development in the concrete during and within the first few days after the concrete is placed. To supplement construction quality in the field, temperature distributions of the concrete structure can be estimated using a numerical scheme of solving a boundary value equation where all the environmental factors (such as air temperature, wind velocity, solar gain, and solar radiation) and cement heat of hydration are considered.

In the heat transfer problem of a newly placed concrete structure, it is necessary to know the rate of heat generated, QH. This important parameter can be measured in adiabatic or heat of solution methods and determined from relative strength-equivalent age relationship. This study presents methods to determine three material properties for the heat of hydration: activating energy, total amount of heat developed, and the degree of hydration.

The purpose of this study is also to correlate measured temperature distributions in a concrete specimen during the hardening process with the results computed from theoretical considerations developed subsequently in sections 2 and 3. Two-dimensional heat transfer models in both plane systems and axisymmetric systems will be used to validate the heat conduction model. Using the model, first, the importance of several parameters will be identified by a parametric analysis. Then, temperature distribution of the cylindrical concrete specimen in the laboratory (which is controlled at constant temperature and constant heat transfer coefficient neglecting solar radiation) was measured and compared with that yielded by the theoretical considerations. Based on test results from a cylindrical concrete specimen in the laboratory, values of concrete conductivity and specific heat are determined and used in a numerical temperature analysis that considers all the environmental conditions in the field. Also, temperature profiles measured from a concrete pavement covered with different curing materials such as white polyethylene plastic sheets are correlated with the test results computed from the program.

1. INTRODUCTION

Fast track paving or accelerated pavement construction refers to the rapid placement of portland cement concrete pavement to facilitate the expedient opening of the pavement to traffic in a specified period of time. The primary factors that influence the minimum time for opening the pavement to traffic are the rate of strength gain of concrete and weather conditions.

Traditional specifications require a minimum curing period of 7 of 14 days before a concrete pavement can be opened to traffic, regardless of the concrete strength. If the curing properties of concrete can be improved so that the concrete reaches design strength in only 24 hours, the pavement may be opened to traffic much sooner, thereby significantly reducing user-delays. However, some quality control procedures with respect to opening criteria may be impacted by the effects of ambient weather conditions on the rate of strength-gain or hydration of the concrete mix.

In some instances, the criteria for opening a newly placed concrete pavement to traffic may not be consistent with the goals of accelerated paving. First, the mix design for fast track concrete may involve the use of additional cement, special rapid hydrating cement, or the addition of an accelerator. These concrete mixes will hydrate at a much greater rate than a conventional concrete paving mixture due to the above noted modifications to the mix design. In addition, conventional testing techniques require frequent breaking of flexural beams to determine the earliest point in time when the concrete mix obtains sufficient strength to meet the opening criteria. This approach may be cumbersome and time-consuming for field personnel to manage effectively. However, non-destructive testing devices (i.e. maturity meters) are available to monitor when the concrete meets the specified opening criteria.

The interaction between temperature conditions in concrete pavement within the first few days after the concrete is placed can influence the quality of the concrete over its lifetime. This means that processes occurring in concrete at an early age have an important influence on concrete quality. Therefore, planning of concrete placement should account for monitoring of the temperature and strength development in the concrete during and within the first few days after the concrete is placed.

Using the maturity concept a correlation between an in-place test method and concrete strength has been established. The in-place test method is involved with field measurement of the in-place temperature history of a concrete pavement section. To supplement construction quality in the field, temperature distributions of the concrete pavement can be estimated using a numerical scheme of solving a boundary value equation where all the environmental factors such as air temperature, wind velocity, solar gain, and solar radiation are considered. Besides these environmental factors, different types of surface protection such as polyethylene sheets and cotton mats can be considered in the modeling process. Since the in-place temperature estimation with the model in performed on large structure (pavement) which experiences higher early-age temperatures than the companion concrete specimens, the heat of hydration must also be considered in the program to accurately estimate temperature distributions of concrete pavement at early ages.

The purpose of this study is to correlate measured temperature distributions in a concrete pavement during the hardening process with the results computed from theoretical considerations developed in Texas Transportation Institute. In order to account for the heat of hydration, a heat transfer analysis of the exothermic phenomenon is considered with heat conduction. Two-dimensional heat transfer models in both plane systems and/or axisymmetric systems will be used to validate

the heat conduction model. The importance of several parameters relative to the significance of climatic conditions, thermal properties, and heat of hydration properties will be identified by a parametric analysis.

Based on test results from a cylindrical concrete specimen in the laboratory (which is controlled at constant temperature and constant heat transfer coefficient neglecting solar radiation), values of concrete conductivity and specific heat are determined and used in a numerical temperature analysis that considers all the environmental conditions in the field. Also, temperature profiles measured from a concrete pavement covered with a different curing material such as white polyethylene plastic sheets are correlated with the test results computed from the program.

2. MODELS FOR TEMPERATURE PREDICTION

Temperature development in concrete due to hydration and ambient temperature conditions can be determined from the general differential equation for heat transfer. The governing equation of heat transfer, due to conduction in a two dimensional domain can be expressed below:

$$\frac{\partial}{\partial x}\left(k_x \frac{\partial T}{\partial x}\right)+\frac{\partial}{\partial y}\left(k_y \frac{\partial T}{\partial y}\right)+Q_H=\rho c_p \frac{\partial T}{\partial t} \qquad (1)$$

where k = thermal conductivity of concrete, W/m · ℃

ρ = concrete density, kg/m^3

c_p = specific heat, J/kg · ℃

t = time, hour

T = temperature, ℃

Q_H= generated heat from heat of hydration of cement, W/m^3

It should be noted that the thermal conductivity of cementitious materials may be expressed using the heat of hydration, α as $k_o(2-\alpha)$ where k_o is a reference conductivity.(*1*)

2.1 Environmental Variables

Heat energy is transferred between a concrete surface and the environment through convection, solar gain, and solar radiation. Figure 1 presents heat transfer between a concrete pavement on the ground and the surrounding environment.

At the concrete surface (Γ_1), heat transfer is affected by all the heat

mechanisms such as wind (convection), solar gain, and solar radiation through the environment. At 1-2 m below bottom of the concrete layer (Γ_2), heat transfer is affected by conduction. These two conditions are summarized as follows:

$$k\vec{\nabla}T \cdot \vec{n} + q_c + q_r - q_s = 0 \ \ on \ \Gamma_1 \tag{2}$$

$$k\vec{\nabla}T \cdot \vec{n} = 0 \ \ on \ \Gamma_2 \tag{3}$$

where q_c = heat flux due to convection, W/m^3

q_r = heat flux due to surroundings, W/m^3

q_s = solar radiation absorption, W/m^3

n = unit direction of heat flow by vector notation

2.1.1 Wind

The flux of heat transfer by convection, q_c, is associated with the movement of air fluid, i.e. wind. The rate of heat transfer by wind is expressed by Newton's law of cooling stated as the heat rate absorbed or dissipated depends on the difference of air temperature, T_e, and the concrete surface temperature, T_s. Also involved in the flux expression is the proportionality constant which is known as the convective heat transfer coefficient, h_c. The appropriate rate equation is of the form:

$$q_c = h_c(T_s - T_e) \tag{4}$$

The empirical convective heat transfer coefficient, h_c, is somewhat complicated

to determine because of the many variables which affect it. It is a complex function of the composition of the air, the roughness of the concrete surface, and the nature of the fluid motion. A typical range of the heat transfer coefficient extends from 5 to 35 $W/m^2 \cdot ℃$.(*1-3*)

Attempts have been made to relate convection heat transfer coefficient to wind velocity of the air and concrete surface roughness.(*4*) It is useful to consider the following empirical formula to estimate a value of h_c:

$$h_c = (6 + 3.7v) \tag{5}$$

A value of 6 $W/m^2 \cdot ℃$ for h_c represents an average concrete surface roughness without any contribution from wind effects. The latter portion of the above expression is added to adjust the value of h_c as a function of wind (m/sec), v.

2.1.2 Solar Gain

In terms of a concrete surface and its distant field surroundings, some incidents of radiation are emitted and absorbed and radiative exchange between the concrete surface and its surroundings takes place. These solar gain rates are affected by a material property of the concrete surface and represented using an emissivity which ranges from 0.8 to 0.9 for the cementitious materials. In general, the Stefan-Boltzmann's law explains solar gain transfer mechanism between a concrete surface and its surroundings as follows:

$$q_r = \varepsilon \sigma (T_s^4 - T_\infty^4) \tag{6}$$

where ε = surface emissivity of concrete

σ = Stefan-Boltzmann constant, 5.670 x 10-8 W/(m^2 · ℃^{4})

T_∞= surrounding temperature, K

2.1.3 Solar Radiation

Solar radiation represents a calculated rate related to the thermal energy that is incident upon a concrete surface. The sun's rays which are absorbed directly by the concrete surface cause the concrete surface to be heated more rapidly than the interior region of a concrete structure. This effect may contribute to a temperature gradient through the pavement.

As discussed before, the important parameters for a heat transfer analysis of a concrete pavement are the thermal properties (conductivity, density, and specific heat), heat transfer coefficient, ambient temperature of the air, solar absorptivity and emissivity. Besides these factors are other important factors such as initial concrete placement temperature and the heat of hydration. Table 1 lists useful information as various input data for heat transfer analysis based on literature review.(*1-3,5-10*) As observed in Table 1, a wide range exists in possible values of concrete thermal conductivity. The coefficients range from 49 to 101 J/cm · ℃ · hr.

3. METHODS TO DETERMINE HEAT OF HYDRATION OF CONCRETE

In the heat transfer problem of a concrete structure, concrete not only conducts heat but also generates heat because of hydration of cement. To solve the heat transfer problem and determine the temperature development, it is

necessary to know the rate of heat generated, Q_H in a unit volume of concrete. This important parameter can be measured in adiabatic or heat of solution methods and determined from relative strength-equivalent age relationship. This section presents methods to determine three material properties for the heat of hydration.

3.1 Basic Relations In Heat of Hydration

The generated heat rate per unit volume and time (heat of hydration) can be expressed as follows(*6*):

$$Q_H = \frac{dW}{dt} \tag{7}$$

where

$$t_e = \Sigma \exp\left[-\frac{E}{R}\left(\frac{1}{T+273} - \frac{1}{T_r+273}\right)\right]\Delta t \tag{8}$$

where W = generated heat of a unit volume of concrete, J/cm^3

H_u = total amount of heat liberated at complete hydration of a unit weight of cement, J/g

C = cement content per unit volume of concrete, g/cm^3

α = degree of hydration

t_e = equivalent age, hr

E = activation energy, J/mol

R = the universal gas constant, 8.3144 J/(mol · ℃)

T_r = reference temperature, ℃ (usually 23 ℃)

The degree of hydration is a function of the equivalent age as follows:

$$\alpha = \exp[-\lambda_1 (\ln \tau)^{-\kappa_1}] \tag{9}$$

where λ_1 and κ_1 are material constants and $\tau = 1+(t_e / t_1)$ using an additional material constant, t_1. It seems that α is over-specified, although Eq. (10) is well-known expression for the degree of hydration commonly used in Europe. Combining above equations, one obtains:

$$Q_H = H_u C \alpha \frac{\lambda_1 \kappa_1}{t_1} \frac{[\ln(\tau)]^{-(1+\kappa_1)}}{\tau} \times \exp\left[-\frac{E}{R}\left(\frac{1}{T+273} - \frac{1}{T_r+273}\right)\right] \tag{10}$$

It is seen from Eq. (11) that the heat of hydration at any equivalent time, t_e, can be calculated from the total amount of heat liberated at complete hydration, H_u, cement content, C, the degree of hydration, α, and the activating energy, E.

3.1.1 Activation Energy

The activation energy can be determined by ASTM test C1074. (*11*) The ASTM standard procedure is based on the relationships of temperature sensitivity and rate of strength gain of cementitious specimens. To determine the activation energy, E, the Arrhenius equation is used as follows:

$$\ln(k_T) = \ln(A) - \frac{E}{R}\frac{1}{(T+273)} \tag{11}$$

According to ASTM 1074, the strength of the mortar cube can be plotted in terms of age at each curing temperature after conducting mortar cube strength tests. The following strength-maturity relationship can be used to determine the

activation energy of a concrete mix:

$$\sigma = \sigma_u \frac{k_T(t - t_o)}{1 + k_T(t - t_o)} \tag{12}$$

where σ is strength at a certain age, σ_u as ultimate strength, k_T as rate constant at curing temperature T, t as curing age at a constant temperature, and t_o as initial age when strength is developed. Least-squares regression analysis is used to determine the values of k_T for the mixture at each curing temperature.

Then, the slope of the line, E/R in Eq. (12) is determined from the natural logarithm of the quotients (k_T values) as a function of the reciprocal absolute temperature. The activation energy, E can be found by multiplying E/R by the universal gas constant, R.

3.1.2 Total Amount of Heat Developed

It is necessary to know the heat produce at complete hydration but it is difficult to determine. According to Emborg(*6*), some researchers have used fictitious value of total amount of heat developed, H_u. This is because it requires at least 2 days or more to obtain adiabatic temperature rise from the adiabatic calorimetry. However, the total amount of heat liberated can be determined easily by the heat of solution method which is described in ASTM C186.(*12*)

3.1.3 Degree of Hydration

Change in the values of the degree of hydration for concretes can be determined by cement samples from the calorimetry. This is what most engineers do. If

cement samples are tested at the isothermal condition, change in their degree of hydration with equivalent time exhibits a S-shape curve. However, the plot in the degree of hydration versus equivalent time has a similar trend to the trend exhibited in the plot of the relative strength curve with equivalent time from the cement mortar tests. Therefore, the degree of hydration in Eq. (10) will be represented by the relative strength data from the cement mortar tests. Least-squares regression analysis is again used to determine the constants of λ_1, t_1, and κ_1.

3.2 Experimental Program for Heat of Hydration

Mortar mix in the laboratory was made to determine activation energy, E, and the degree of hydration, α which is composed of three constants of λ_1, t_1, and κ_1. Also, a cement sample was used to determine total amount of heat, H_u, developed by the heat of the solution method.

3.2.1 Mix Designs and Specimen Preparation

Table 2 shows the concrete mixtures proportions. However, the mortar mixture for the mix design had cement-to-sand proportions equal to the cement-to-coarse aggregate proportions in the concretes.(*13*) According to Carino (*13*), the activating energy determined from concretes is pretty similar to the value determined from the mortar mixture whose mix design had cement-to-sand proportions equalto the cement-to-coarse aggregate proportions in the concretes. Thus for an experimental program in our work only mortar mixture was used.

Mortar cube specimens were prepared using the brass mold which has three 51 mm cube compartments. All the specimens were demolded at the time of the first strength test and cured into temperature-controlled water baths until the day of testing.

3.2.2 Tests and Data Analysis

The strength-age data for each mixture were used to determine the parameters of the strength-age relationship in Eq. (13). From those strength-age data, each constant of k_T at each isothermal condition in Eq. (13) are determined by the regression analysis and given in Table 3. Using the relations of the rate constant, k_T and curing temperature, T, value of activation energy, E was obtained using Eq. (12). Table 3 lists activation energy value as 47.8 kJ/mol. Presently, there is not much published data on the effect of activation energy of mortars which contain different replacement of cement by fly ash. Carino and Tank (*13*) reported 40-60 kJ/mol of activating energy for mortar specimens made with Type I cement.

Next, the empirical coefficients of Eq. (10) were determined by the relative strength data of the cement mortar tests, using the least squares analysis. The three coefficients of λ_1, t_1, and κ_1 represent the shape factor for the degree of hydration for the concrete mixture. Table 3 summarizes the values of λ_1, t_1, and κ_1 for the mix. The degree of hydration versus equivalent age values, obtained using Eq. (10), is shown in Fig. 2. There is relatively good agreement between the degree of hydration equation (Eq. (10)) and the data.

Finally, the total amount of heat liberated, H_u was determined using the isothermal calorimeter (heat of solution method). As seen in Table 3, test value was 483.0 J/g. This value is reasonable since it was noted that Type I cement has average value of 497 J/g.(*14*)

4. PREDICTION OF TEMPERATURE DISTRIBUTION

The purpose of this section is to correlate measured temperature distributions

in a concrete pavement during the hardening process with the results computed from theoretical considerations developed in sections 2 and 3. In order to account for the heat of hydration, a heat transfer analysis of the exothermic phenomenon is considered with heat conduction. Two-dimensional heat transfer models in both plane systems or axisymmetric systems will be used to validate the heat conduction model. As discussed before, the importance of several parameters will be identified by a parametric analysis. Based on test results from a cylindrical concrete specimen in the laboratory (which is controlled at constant temperature and constant heat transfer coefficient neglecting solar radiation), values of concrete conductivity and specific heat are determined and used in a numerical temperature analysis that considers all the environmental conditions in the field. Also, temperature profiles measured from a concrete pavement covered with a different curing materials such as white polyethylene plastic sheets are correlated with the test results computed from the program.

4.1 Sensitivity Analysis of Heat Transfer in Concrete Structure

In order to study the significance of the various parameters, temperature change at the surface of a concrete pavement (Fig. 3) was calculated. By keeping the rest of the variables in Table 4, one variable at a time was increased by 10 percent.

A summary of comparisons is given in Table 5. It can be seen that the most significant factors with respect to the environmental variables are air temperature and initial concrete temperature. Also of importance is the absorptivity of the surface to the solar radiation.(5) However, an increase in the thermal conductivity, specific heat, and density of concrete reduces the temperatures at

the concrete surface.(*5*) An increase in the thermal conductivity, specific heat, and density of soil does not seem to change the temperature at the concrete surface.

With respect to the heat of hydration of cement properties, an increase in the total amount of heat developed, H_u, the cement content, C, and the activating energy, E does not amplify the predicted temperature at the concrete surface. However, material constants of the degree of hydration properties such as λ_1, t_1, and κ_1 decrease the temperature at the concrete surface by 1.2 %, 1.0 %, and 0.5 %, respectively.

4.2 Experimental Temperature Distribution of Cylindrical Specimen

A cylindrical concrete specimen (diameter=26.0 cm and height=25.4 cm) was prepared with thermocouples at five different locations along the axis of the specimen in the laboratory. The laboratory was controlled by constant room temperature (32 ℃). The mix design (in Table 2) was used as the concrete materials. Five channels in the data logger were used to record the temperature at five different depths in the cylinder: 2.54 cm (1 inch), 7.62 cm (3 inches), 12.7 cm (5 inches), 17.8 cm (7 inches), 22.9 cm (9 inches), and room temperature. The measurement time interval was 30 minutes.

This analysis uses a two-dimensional axisymmetric heat transfer model. The finite element mesh is shown in Fig. 4. In this analysis, a half model of the total structure is used to take advantage of symmetry along the center line axis.

Adiabatic temperature conditions are assumed to exist at the boundary condition on the axis and can be defined:

$$k\vec{\nabla}T \cdot \vec{n} = 0 \tag{13}$$

For the other surfaces, the mixed boundary condition is applied as follows:

$$k\vec{\nabla}T \cdot \vec{n} + h_c(T_s - T_e) = 0 \tag{14}$$

The top surface is exposed to an ambient temperature of 32 ℃, and the convective heat transfer coefficient of 4 J/cm^2 · hr · ℃. For the right-hand side vertical surface, the heat transfer coefficient of 2 J/cm^2 · hr · ℃ is applied. On the bottom surface, the heat transfer coefficient is 0.5 J/cm^2 · hr · ℃. Based on experimental research, the cement heat of hydration characteristics which were determined from concrete mix are used as input data (Table 3). However, a total amount of heat liberated at complete hydration H_u was used as 440.3 J/g instead of 483.0 J/g since the mix contains 21 percent of Type C fly ash and fly ash liberates less heat. It should be noted that the laboratory samples (cement samples for the heat of solution method) did not contain fly ash. In the analysis, a time increment of 0.1 hours was selected. An initial temperature of 19 ℃ was used for the analysis.

Figure 5 shows temperature measurements of the concrete cylinder specimen at various different locations. The maximum temperature at 2.54 cm (1 inch) below the top surface (called top 2.54 cm, for brevity) was 37.4 ℃ after 23.5 hours. On the other hand, the maximum temperature at 2.54 cm above the bottom surface (called bottom 2.54 cm) was 41.3 ℃ after 20.5 hours. Between the top 2.54 cm and bottom 2.54 cm, temperature gradient was 3.7 ℃.

The predicted concrete temperatures at the five different depths (which are the same depths as for the experiments) are shown in Fig. 6. From the analysis,

maximum temperatures occurred at 23.5 hours and were 39.4 ℃ and 41.8 ℃ at the top 2.54 cm and the bottom 2.54 cm, respectively. The comparison between measured and predicted temperatures was found to be satisfactory. Based on test results, concrete conductivity was $45(2-\alpha)$ J/cm • hr • ℃ where α being the degree of hydration and concrete specific heat as 1.05 J/g • ℃.

4.3 Experimental Temperature Profiles of Concrete Pavement

The test sections in Harris County (Cypress in Texas) were placed during August, 1993. These test sections are comprised of 33.0 cm (13 inches) thick continuously reinforced concrete pavement consisting of different curing conditions. Different curing methods were used to control the drying process of the concrete. Two different curing methods were employed in these experimental sections as follows:

(i) Membrane curing compound, which is called the standard curing method;

(ii) Polyethylene film curing, plus membrane curing, called Polyethylene for brevity.

The concrete pavement section had two layers of reinforced steel with #5 steel as the longitudinal rebars and #6 steel as the transverse rebars. The top layer of transverse rebars was placed at the mid-depth of the pavement; and the bottom layer of transverse rebars was 6.5 cm (2.5 inches) above the surface of the soil. The addition of steel rebars will increase the thermal conductivity of the concrete pavement systems.

The test section was placed at 9:00 A.M., August 20, 1993. Figure 7 illustrates the air temperatures used for input. The air temperatures ranged from

19 to 31 ℃ in the first day. The solar radiation and wind velocity are shown in Fig. 8. The maximum solar radiation was 0.923 kW/m^2 while the maximum wind velocity was 1.8 m/sec in the first day.

The initial soil temperature was assumed to be 21 ℃. As an initial concrete temperature, 25 ℃ was used. To have better fit values to experiments, different hydration parameters are assumed while the total heat developed, H_u, cement content, C, and the activating energy, E, are kept unchanged (See Appendix D of reference *16*).

Figures 9 to 11 show the measured and numerically calculated temperatures of the actual concrete pavement structure. The maximum measured temperature was 43.6 ℃ (along 2.54 cm from the pavement surface), 49.3 ℃ (along the middle depth of concrete), 48.0 ℃ (along 2.54 cm from the concrete bottom surface). After about 12 hours, the concrete temperature around the top surface fell at a uniform rate. However, the concrete temperatures at the middle depth and the bottom surface still increased until 15 hours after the start of construction. The maximum temperatures were predicted to be 44.7 ℃ (along 2.54 cm from the pavement surface), 48.7 ℃ (along the middle depth of concrete), 48.9 ℃ (along 2.54 cm from the concrete bottom surface). As Figures 9 to 11 show, predicted temperature trends at the top surface did not match well to the measured temperatures until after the maximum temperatures were reached, probably resulting from the effect of membrane curing materials, or hydration of cement properties, or possibly uncalibrated weather station data.

The second example incorporates a polyethylene cover as insulating materials. Two series of tests were made. In the first series, temperatures of the concrete pavement section (membrane curing only) were monitored and analyzed before.

In the second test series, the polyethylene sheets were covered after 24 hours of construction to determine the heat retention.

The same input data was used for the polyethylene-covered concrete section, except for different boundary conditions applied at the top concrete surface. The coefficient of solar radiation absorption, α_s =0.6 was used and the following convective heat transfer coefficient, h_c was used:

$$h_c = 1.563(v)^{0.237} \tag{15}$$

where v is wind velocity as mph (1 mph = 0.4471 m/s).

The corresponding time-temperature curves are shown in Fig. 12. The pavement section covered with polyethylene film was subjected to a greenhouse effect, which made the temperature in the pavement cured with the standard curing method.(*15,16*) For the standard curing method, maximum temperature at 2.54 cm below the concrete surface was measured as 47.3 ℃ while the model predicts 50.4 ℃ at the second construction day. On the other hand, for the polyethylene-covered section, maximum temperature at 2.54 cm below the concrete surface was measured as 55.2 ℃ while the model predicts 57.2 ℃ at the second construction day. Although calculated temperature was seemed to be higher than the measured one from both two different curing sections, the comparison was found to be satisfactory.

5. CONCLUSIONS

The following conclusions and recommendation could be made from this study:

1. This study provides a concise review of current information and knowledge

of several significant factors affecting the development of temperature and heat of hydration as it would pertain to hardening concrete pavement materials.

2. Several parameters relative to the characterization of climatic conditions (convection, solar gain, and solar radiation) were identified. Although limited information is available for the transfer of heat by convection and solar gain, the relationships provided in the text of this study provide the necessary input in which to assign values to these parameters for the analysis portion of this study. The importance of those variables in the overall analysis has been addressed by the parametric analysis.

3. The cement hydration characteristics can be determined by the solution method. Three necessary material properties such as the activating energy, E, total heat liberated, H_u, and the degree of hydration, α, can represent the internal heat generation of the heat transfer equation. In this study, the activating energy and the degree of hydration curve are determined well from the mortar compressive strength tests while total amount of heat liberated from the hydration of the cement is determined by the isothermal calorimeter method. For future work, activation energy of mortars containing fly ash, slag and/or silica fume should be considered with different types of cements.

4. A concrete pavement structure is unlike most other structures because they possess very large surface to volume ratios causing significant variations in temperature and moisture. As a result, thermal properties such as concrete conductivity or thermal diffusivity would affect the heat transfer of the concrete pavements at an early age. Thus, concrete conductivity can be back-calculated from the best fit value between the computed and measured

laboratory process with a cylindrical specimen. Then, temperature distribution of the newly placed concrete pavement on the ground can be accurately predicted with environmental data by the theoretical considerations.

5. To increase concrete curing temperature, insulating materials such as polyethylene sheets, cotton mat, or blankets can be used. The insulation used typically depends on the climatic conditions. Based on historic experiments, heat loss by convection can be represented by several different functions in terms of wind velocity for different curing materials. Specially, solar radiation absorptivity can be increased as the polyethylene sheets are covered on the concrete pavement sections.

Tables

Table 1 Concrete Thermal Properties and Heat Transfer Coefficient from Others (*1-3, 5-10*)

Table 2 Mix Design (1 m^3 of Concrete)

Table 3 Input Data for Heat of Hydration

Table 4 Input Data for Parametric Analysis

Table 5 Parametric Study Results (Weather Data from Waller County in Texas was Used)

Table 1 Concrete Thermal Properties and Heat Transfer Coefficient from Others (*1-3, 5-10*)

Source	Conductivity (J/cm · ℃ · hr)	Specific Heat (J/g · ℃)	Heat Transfer Coefficient (J/cm^2 · ℃ · hr)	
Hsieh	48.6	0.905	Winter	12.3
			Summer	8.2
			Free	1.8
Emborg	57.6-90	0.8-1.2		-
Truman	73.1	0.879	with form	1.7
			w/o form	8.3
Johnson	50.5	0.963		4.01
Brebbia	50.4	0.96	Top	8.28
			Bot	2.52
			Left	5.40
			Right	3.24
			Inside	0.72
Machida	72.1	0.983	Room	3.77
Tan	79-101	-		-
Rastrup	-	1.07		-
Chapmann	61.2	0.81		-

Table 2 Mix Design (1 m^3 of Concrete)

Material	Weight or Volume
Cement, type I	251
Fly ash, type C	68
Crushed limestone	684
Siliceous sand 1	399
Siliceous sand 2	765
Water	135
Concrete unit weight	2301 kg/m^3

Table 3 Input Data for Heat of Hydration

T (℃)	k_T (1/day)	E (kJ/mol)	λ_1	t_1	κ_1	H_u (J/g)
10	.153					
25	.389	47.8	1.65	13	1.21	483
50	1.867					

Table 4 Input Data for Parametric Analysis

	Input data	Values
Concrete	k, (J/cm · hr · ℃)	61.1 (2- α)
	ρ, (g/cm^3)	2.357
	c_p, (J/g · ℃)	1.044
	α_s	0.5
	ε	0.9
Soil	k, (J/cm · hr · ℃)	50.0
	ρ, (g/cm^3)	1.632
	c_p, (J/g · ℃)	0.800
	α_s	0.5
	ε	0.9
Heat of hydration of cement	H_u, (J/g)	440.3
	C, (g/cm^3)	0.32
	E, (J/mol)	47755
	λ_1	1.65
	t_1	13
	κ_1	1.21

Table 5 Parametric Study Results (Weather Data from Waller County in Texas was Used)

Variables	% ΔT at top
Concrete k	-0.7
Concrete c_p	-1.3
Concrete ρ	-1.3
Soil k	0.0
Soil c_p	0.0
Soil ρ	0.0
Air temperature	4.7
Wind velocity	-0.6
Solar absorptivity	3.2
Emissivity	-0.5
Initial concrete temp.	3.4
Initial soil temp.	0.5
Thickness of slab	0.0
H_u	0.5
C	0.5
E	0.7
λ_1	-1.2
t_1	-1.0
κ_1	-0.5

Figures

Fig. 1 Heat Transfer Between a Concrete Surface and the Environment

Fig. 2 Degree of Hydration Versus Equivalent Age

Fig. 3 Typical Concrete Slab Idealization in 2-D Model

Fig 4 Concrete Cylinder and Meshes in the 2-D Axisymmetric Model

Fig. 5 Measured Concrete Temperatures from the Cylinder (Laboratory)

Fig. 6 Predicted Concrete Temperatures from the Cylinder

Fig. 7 Hourly Air Temperatures (Harris County, TX, August 20-22, 1993)

Fig. 8 Hourly Solar Radiation and Wind Velocity (Harris County, TX, August 20-22, 1993)

Fig. 9 Temperature History at 2.54 cm from the Top Surface of the Concrete Pavement

Fig. 10 Temperature History at the Middle Depth of the Concrete Pavement

Fig. 11 Temperature History at 2.54 cm from the Bottom Surface of the Concrete Pavement

Fig. 12 Temperature History at 2.54 cm from the Top Surface of the Concrete Pavement (Two Different Curing Sections)

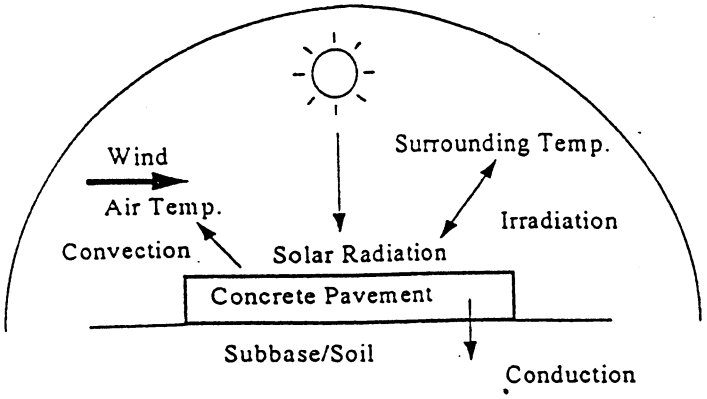


Fig. 1 Heat Transfer Between a Concrete Surface and the Environment

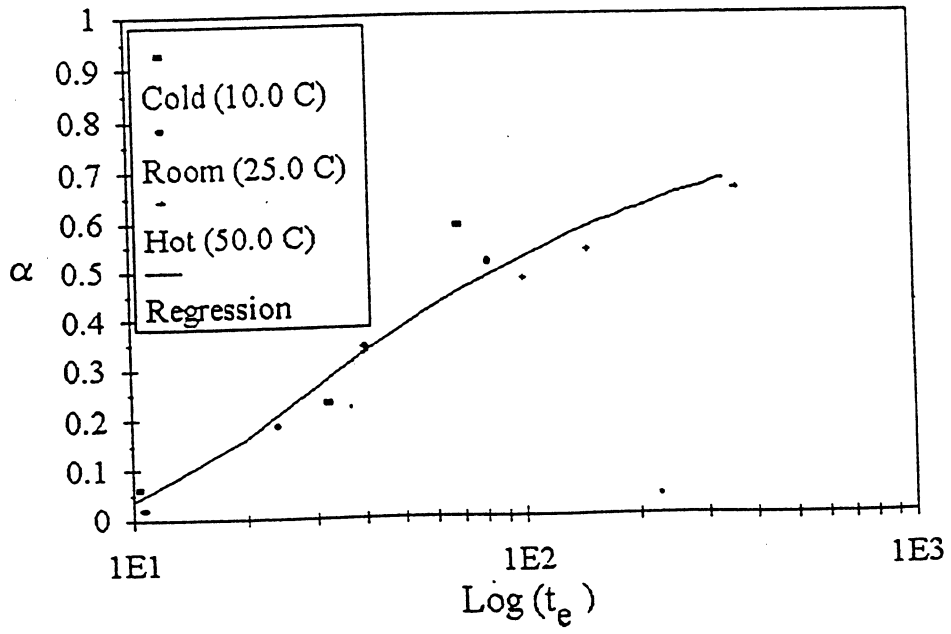


Fig. 2 Degree of Hydration Versus Equivalent Age

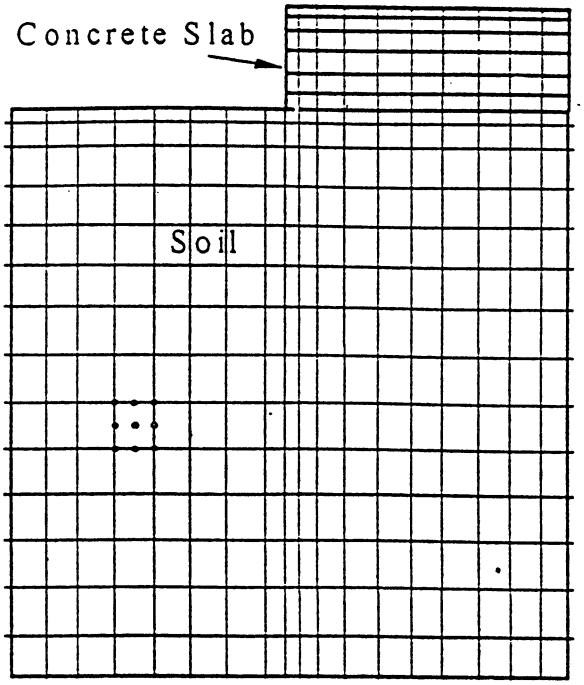


Fig. 3 Typical Concrete Slab Idealization in 2-D Model

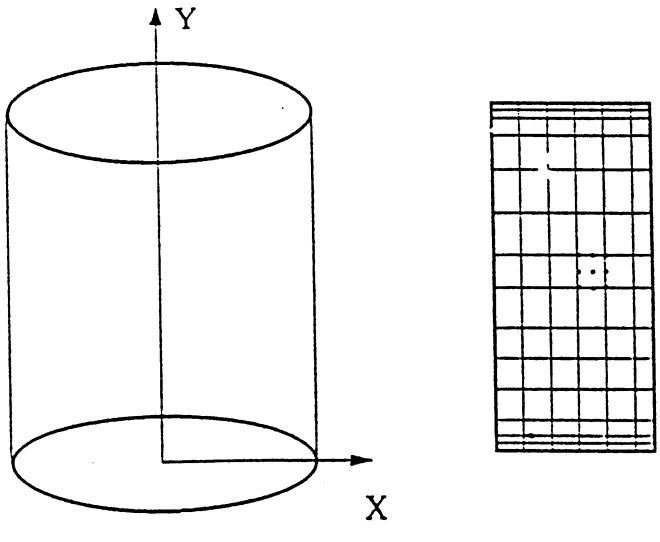


Fig 4 Concrete Cylinder and Meshes in the 2-D Axisymmetric Model

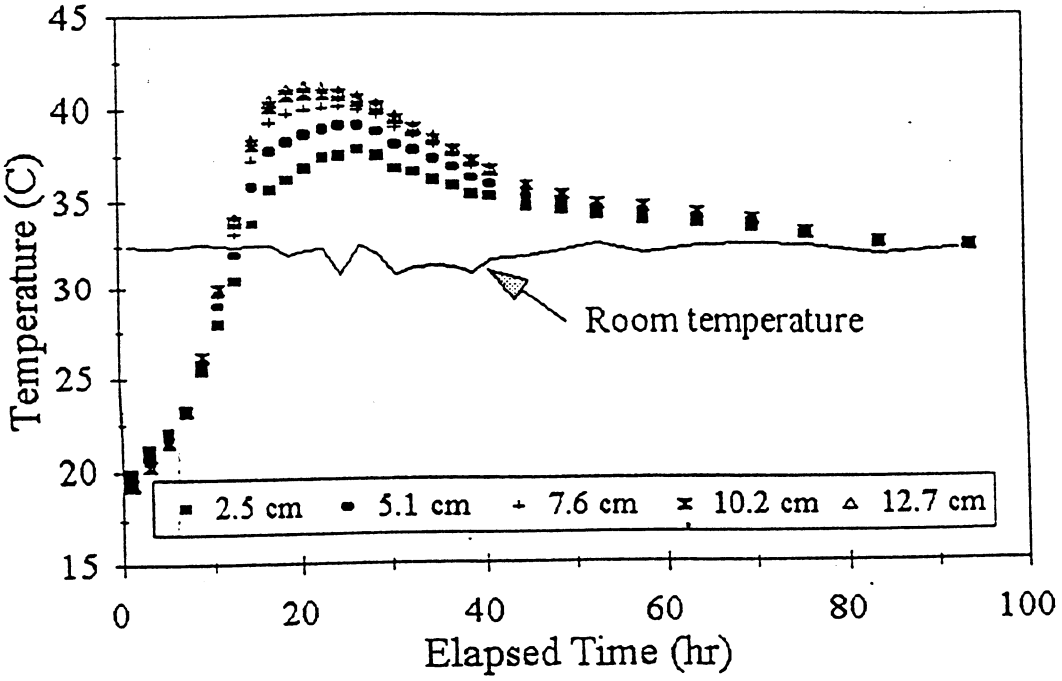


Fig. 5 Measured Concrete Temperatures from the Cylinder (Laboratory)

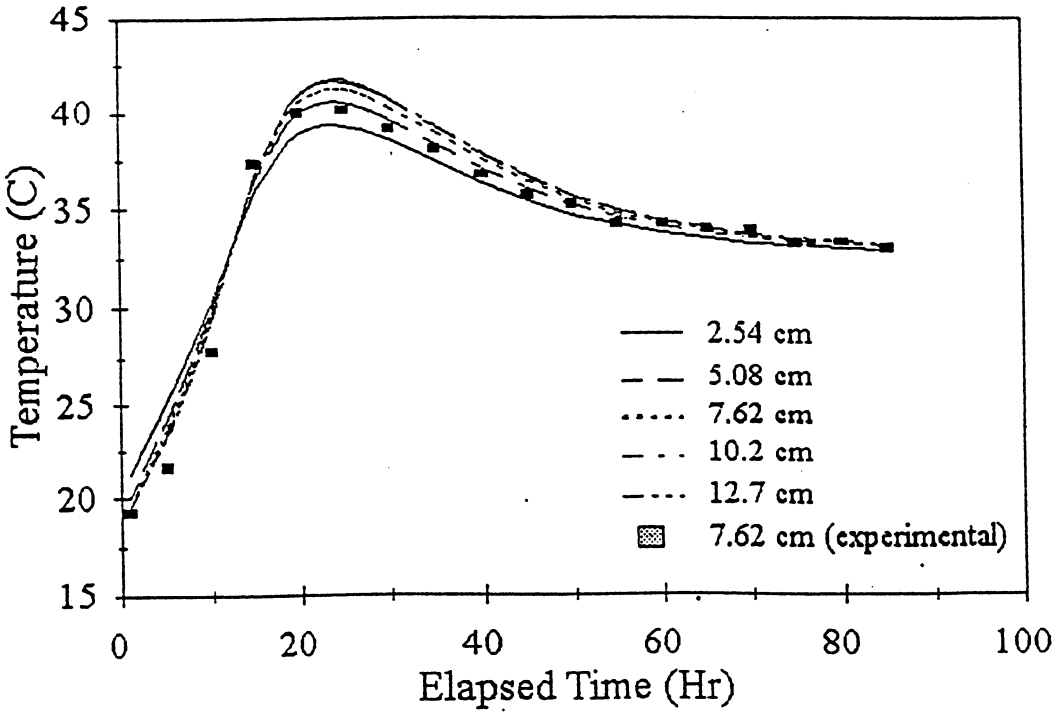


Fig. 6 Predicted Concrete Temperatures from the Cylinder

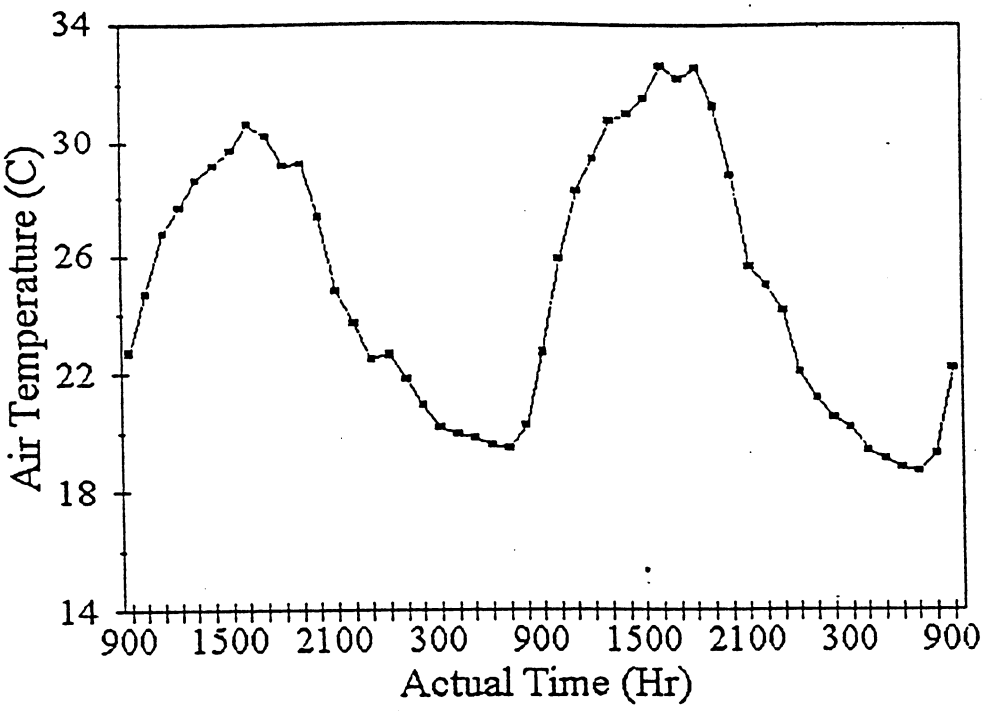


Fig. 7 Hourly Air Temperatures (Harris County, TX, August 20-22, 1993)

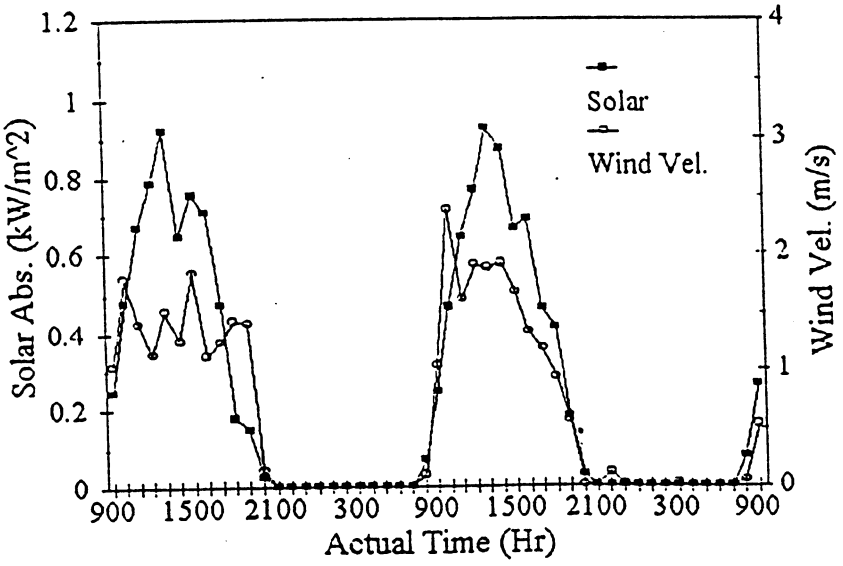


Fig. 8 Hourly Solar Radiation and Wind Velocity (Harris County, TX, August 20-22, 1993)

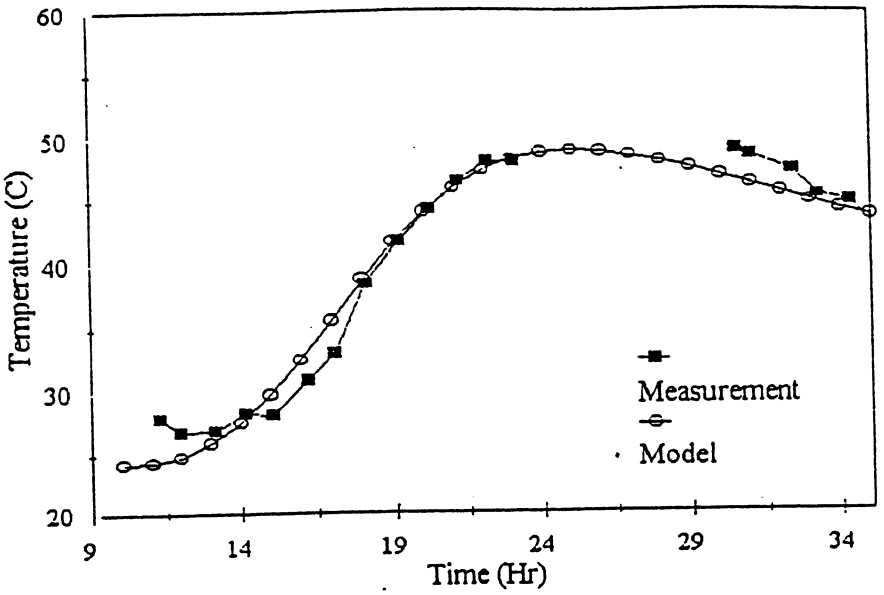


Fig. 9 Temperature History at 2.54 cm from the Top Surface of the Concrete Pavement

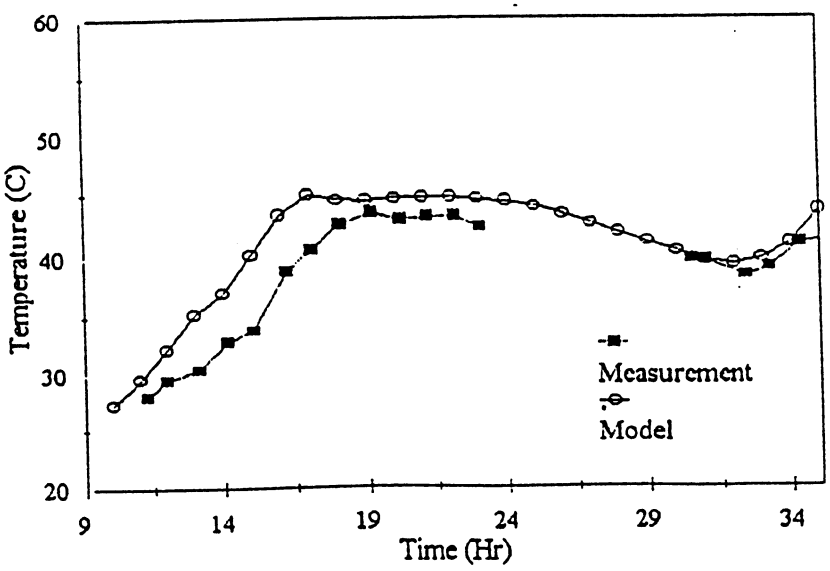


Fig. 10 Temperature History at the Middle Depth of the Concrete Pavement

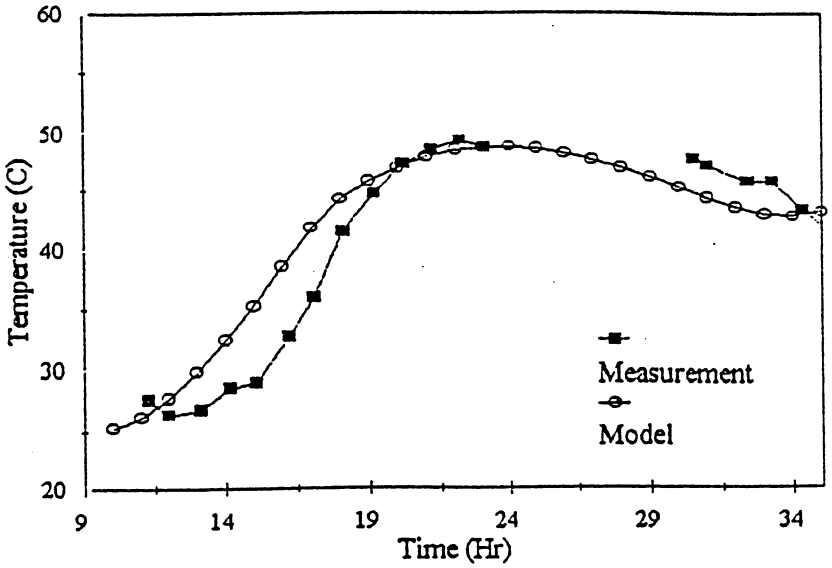


Fig. 11 Temperature History at 2.54 cm from the Bottom Surface of the Concrete Pavement

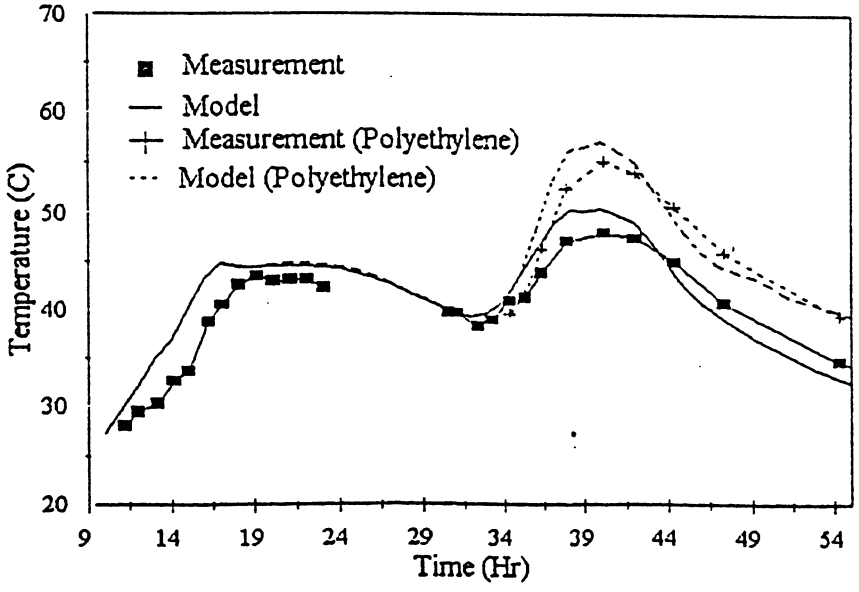


Fig. 12 Temperature History at 2.54 cm from the Top Surface of the Concrete Pavement (Two Different Curing Sections)

REFERENCES

1. Hsieh, C. K., and C. Qin, and E. E. Ryder. Development of Computer Modeling for Prediction of Temperature Distribution inside Concrete Pavements. Report FL/DOT/SO/90-374. Mechanical Engineering Department, University of Florida, Gainesville, 1989.

2. Chapman, A. J. Fundamentals of Heat Transfer. Macmillian Inc., New York, 1982.

3. Rastrup, E. Heat of hydration in concrete. Magazine of Concrete Research, Vol. 6, No. 17, 1954, pp. 79-92.

4. Branco, F. A., and R. A. Mendes, and E. Mirabell. Heat of Hydration Effects in Concrete Structures. ACI Materials Journal, Vol. 89, No. 2, 1992, pp. 139-145.

5. Thepchatri, T., and C. P. Johnson, and H. Matlock. Prediction of Temperature and Stresses in Highway Bridges by a Numerical Procedure using Daily Weather Reports. Center for Transportation Report 23-1. The University of Texas at Austin, 1977.

6. Emborg, M. Thermal Stresses in Concrete Structures at Early Ages. Doctoral Thesis. Lule Univ. of Technology, Sweden, 1989.

7. Truman, K. Z., and D. T. Petruska, and C. D. Norman. Creep, Shrinkage, and Thermal Effects on Mass Concrete Structure.. Journal of Engineering Mechanics, Vol. 117, No. 6, 1991, pp. 1274-1288.

8. Brebbia, C.A. Proc., 6th International Conference, on Board the Liner, the Queen Elizabeth 2, Southampton to New York, Springer-Verlag, New York, 1984, pp. 1-22.

9. Machida, N., and K. Uehara. Nonlinear Thermal Stress Analysis of a Massive Concrete Structure. Computers & Structures, Vol. 26, No. 1/2, 1987, pp. 287-296.

10. Tan, S., and B. Low, and T. Fwa. Thermal Properties of Concrete from Transient Conduction of a Thin Slab. Cement, Concrete, and Aggregates, ASTM, Vol. 14, No. 2, 1992, pp. 78-85.

11. Standard Practice for Estimating Concrete Strength by the Maturity Method. In Annual Book of ASTM Standards, Vol. 04.02, Philadelphia.

12. Standard Test Method for Heat of Hydration of Hydraulic Cement. In Annual Book of ASTM Standards, Vol. 04.01, Philadelphia.

13. Carino, N.J. and R.C. Tank. Maturity Functions for Concretes made with Various Cements and Admixtures. ACI Materials Journal, Vol. 89, No. 2, 1992, pp. 188-196.

14. Breugel, K.V. Simulation of Hydration and Formulation of Structure in Hardening Cement-Based Materials. Delft University of Technology, Netherlands, 1991.

15. Johnson, J., and D. G. Zollinger, and S. Yang. Guidelines for the Construction of Fast Track Concrete Pavement Intersections. Report 1385-1F. Texas Transportation Institute, Texas A&M University, 1993.

16. Yang, S. A temperature Prediction Model in New Concrete Pavement and a New Test Method for Concrete Fracture Parameters. Doctoral Dissertation, Texas A&M University, 1996.